Bull. Chem. Soc. Jpn., 77, 189–193 (2004) 189

pH Dependence of Interparticle Coupling for Gold Nanoparticle Assemblies Formation: Electrostatic Attraction and Hydrogen Bonding

Chia-Hao Su, Pei-Lin Wu,* and Chen-Sheng Yeh*

Department of Chemistry, National Cheng Kung University, Tainan, Taiwan 701, R.O.C.

Received April 24, 2003; E-mail: csyeh@mail.ncku.edu.tw

With the addition of ω-sulfanylalkanoic or ω-alkyldisulfanylalkanoic acids to sodium-contained aqueous Au colloidal solutions, close-packed self-assembly occurred UV–vis, TEM, solid-state ^{13}C NMR, and FT-IR spectra were employed to study the resulting aggregation arrays. The resulting two-dimensional Au assemblies exhibited interparticle coupling via both hydrogen bonding and electrostatic interactions at pH 6. Either acidic (pH 3) or base (pH 11) generated significant three-dimensional close-packed aggregates. It is suggested that electrostatic interactions might lead to the aggregates during the dry-up process in the preparation of TEM samples of the Au nanoparticles capped with COO^- terminals at pH 11. For the acidic solutions (pH 3), coagulation was governed by hydrogen-bonding forces.

Nanostructured materials have given rise to a wide variety of catalytic, optoelectronic, and biomedical applications.[1,2] Using nanocrystallites as building blocks to form large self-assembled and self-organized architectures is an important strategy in nanometer-size device fabrication. Such closely packed assemblies provide the opportunity for optimizing electronic and optical performance with respect to function modulation. Hydrophobic alkanethiols have often been utilized to induce nanoparticles toward self-organization through van der Waals interactions when constructing nanostructural arrays in solutions.[3] Another approach for generating two- (2D) or three-dimensional (3D) aggregates is to make use of hydrogen bonds.[4] Electrostatic coupling is the other non-covalent force used to form the linkages between like-charged particles. Compared with both hydrophobic and hydrogen-bonding interactions, only a handful of closely-packed structures have demonstrated the existence of electrostatic attractions among nanoparticles.[5–7]

A notable feature of metal nanoparticles capped with carboxylic acid- (–COOH) or carboxylate-terminated ($–COO^-$) thiolates is water-solubility. Nanoparticles fabricated with biocompatible properties are an important concept in biotechnology applications. Carboxylic acids have been successfully functionalized onto hydrophobic quantum dots to achieve bioconjugates.[8,9] This methodology has been developed to synthesize dispersed carboxylic acid- or carboxylate-capped metal nanoparticles.[4a–c,6,7,10–13] For example, exchange reactions were performed to substitute the ω-carboxylic acid alkanethiols for the hydrophobic alkanethiolates in the formation of these water-soluble nanoparticles.[4a–c] Kimura and co-workers developed a methodology to prepare water-soluble gold nanoparticles functionalized with carboxylate groups.[11,12] The development of 2D or 3D arrays utilizing carboxylate- or carboxylic acid-modified Au colloids was reported, as well. The groups of both Rotello and Zhong studied the assemblies of the amphiphilic Au nanoparticles showing –COOH functionalities as hydrogen-bonding sites in building nanocrystal aggregations.[4a,b] Adachi reported that the $–COO^-$ terminals facilitated Au nanospheroid assemblies through electrostatic attraction.[6]

It is known that either electrostatic interaction or hydrogen-bonding has been *individually* employed to construct desired assemblies. In this study, we demonstrated that ω-sulfanylalkanoic or ω-alkyldisulfanylalkanoic acids can be mixed with Au colloidal solutions to result in functionalized Au colloids exhibiting both bonding properties, electrostatic and/or hydrogen-bonding interactions, to develop self-assembled architectures. The closely packed 3D arrays were observed in the presence of either electrostatic attractions ($pH = 11$) or hydrogen bonds ($pH = 3$). The formation of 2D self-assembled structures was attained in the presence of both electrostatic and hydrogen-bonded coupling ($pH = 6$).

Results and Discussion

The gold nanoparticles prepared according to Natan's method were 13 ± 1.5 nm in size.[14] When 5 mL of the gold colloidal solution was mixed with 1.1 mmol of $HS(CH_2)_nCOOH$ or $EtSS(CH_2)_nCOOH$ ($n = 10$, 15), a concentration of 7.4×10^{12} particles mL^{-1} was estimated on the basis of the average particle diameter and the $HAuCl_4$ concentration.[15]

When ω-sulfanylalkanoic or ω-alkyldisulfanylalkanoic acids were added to the Au colloidal solutions, the suspensions remained red in color. Figure 1 shows a typical example of the UV–vis absorption. As can be seen, the distinct characteristic Au plasmon band at 520 nm of the dispersed Au particles appears broadened, and increased in intensity after adding $HS(CH_2)_{10}COOH$. This might indicate the formation of Au aggregates. It should be mentioned that the prepared Au particles from Natan's method exhibited a dispersed morphology. TEM images show the 2D arrays distributed as isolated domains accompanied with the dispersed particles on the grids from the resulting solutions, as observed in Fig. 2.

Figure 3 displays the higher magnification TEM micrographs corresponding to $HS(CH_2)_nCOOH$ and $EtSS(CH_2)_n$-COOH ($n = 10$, 15) functionalized Au nanoparticles. The pH was measured at 6 for those solutions. As seen in the TEM,

Published on the web January 13, 2004; DOI 10.1246/bcsj.77.189

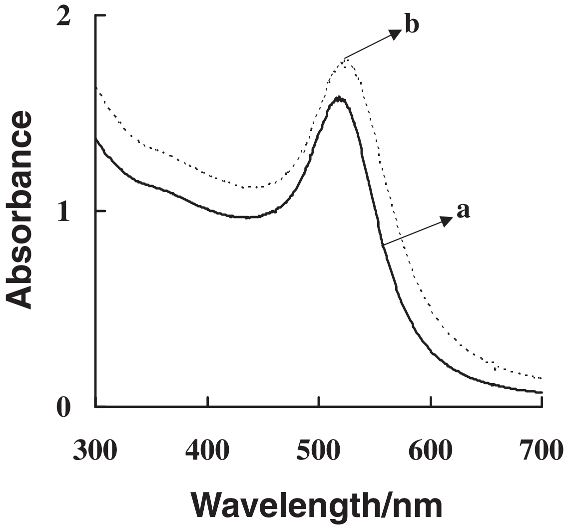

Fig. 1. UV–vis absorption spectra of (a) Au colloidal solution and (b) Au/HS$(CH_2)_{10}$COOH colloids.

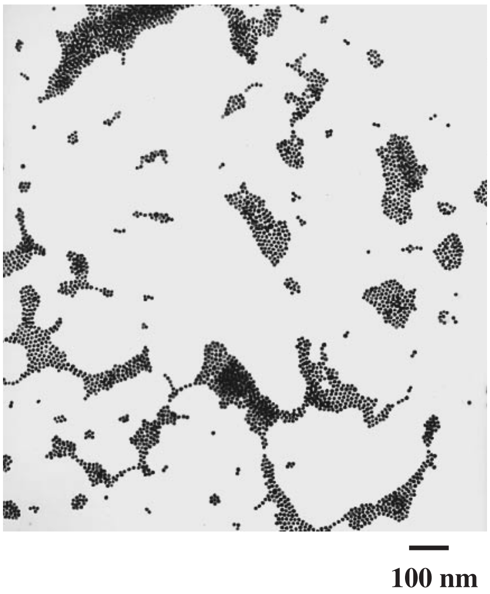

Fig. 2. TEM images of Au/HS$(CH_2)_{10}$COOH colloids at pH 6.

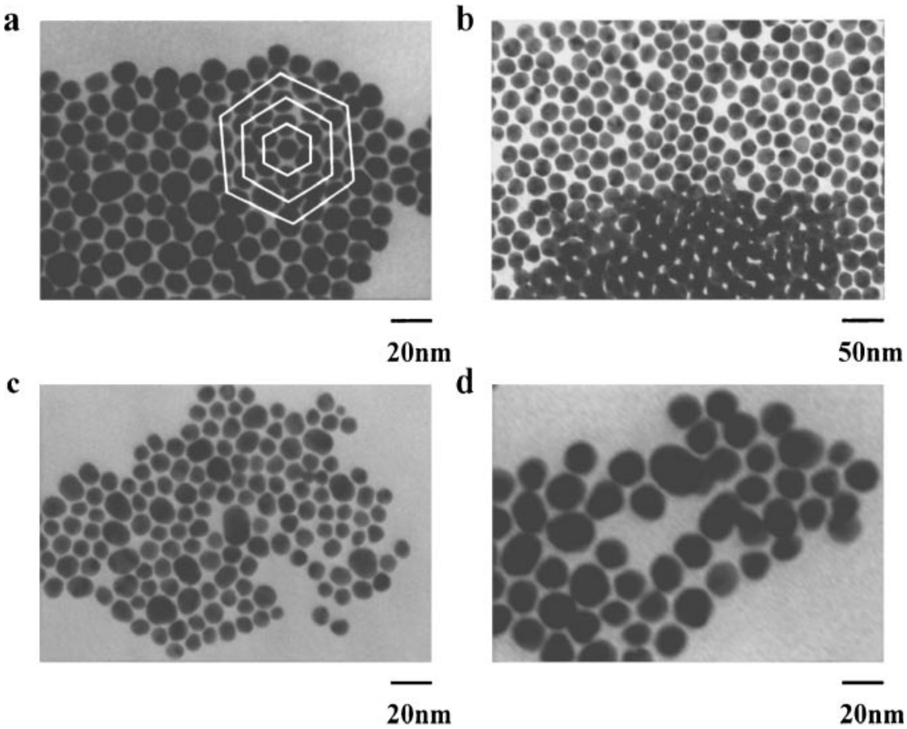

Fig. 3. TEM images of (a) Au/HS$(CH_2)_{10}$COOH, (b) Au/EtSS$(CH_2)_{10}$COOH, (c) Au/HS$(CH_2)_{15}$COOH, and (d) Au/EtSS$(CH_2)_{15}$-COOH colloids. All samples were controlled at pH 6.

the Au nanoparticles organized into regularly ordered 2D monolayers exhibiting a local hexagonal order. Some arrays revealed a 3D assembly leading to cross-linked networks. Those colloidal arrays exhibited an interparticle distance dependence corresponding to the length of the alkyl chain of mercaptocarboxylic acid. For example, the distances between the nanoparticles were evaluated to be 2.0 nm for Au/HS$(CH_2)_{10}$COOH and 2.7 nm for Au/HS$(CH_2)_{15}$COOH assemblies at pH 6. It is known that chemisorption of alkanethiols on gold surfaces leads to the formation of metal–sulfur bonding.[16] Solid-state ^{13}C NMR spectroscopy provided the evidence of the thiolate bonding by investigating Au/HS$(CH_2)_{10}$COOH colloids (pH 6). As seen in Figs. 4a and 4b, no residual trisodium citrate remained in the nanocrystal assemblies based on the disappearance of the carbon signal at 76 ppm. This indicates that the contribution of the trisodium citrate to formation of the organized arrays is negligible. Furthermore, the feature (C11) at 24 ppm (Fig. 4c) was not found in Fig. 4a. The excess ω-sulfanylalkanoic acids were washed out completely. On the contrary, the C11 signal was shifted downfield to 52 ppm, the so called

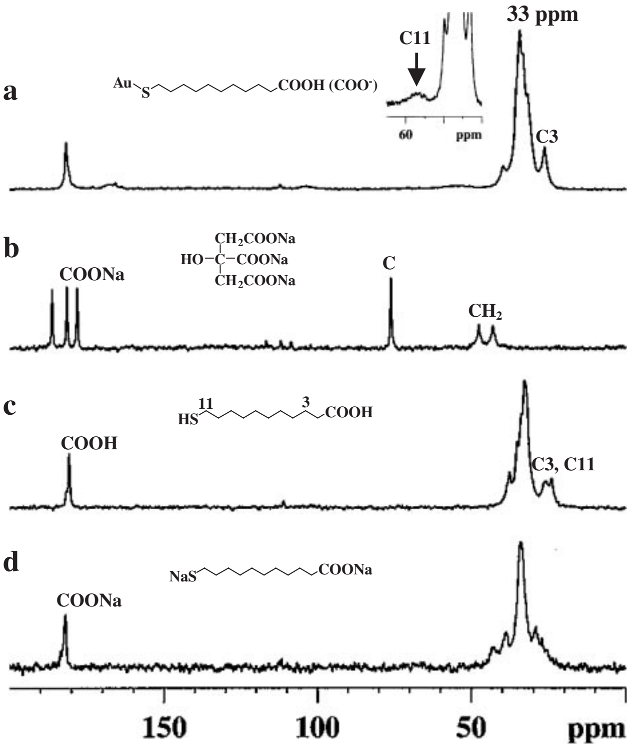

Fig. 4. Solid-state ^{13}C NMR spectrum of (a) Au/HS-$(CH_2)_{10}$COOH at pH 6, (b) trisodium citrate, (c) HS-$(CH_2)_{10}$COOH, and (d) $NaS(CH_2)_{10}COONa$.

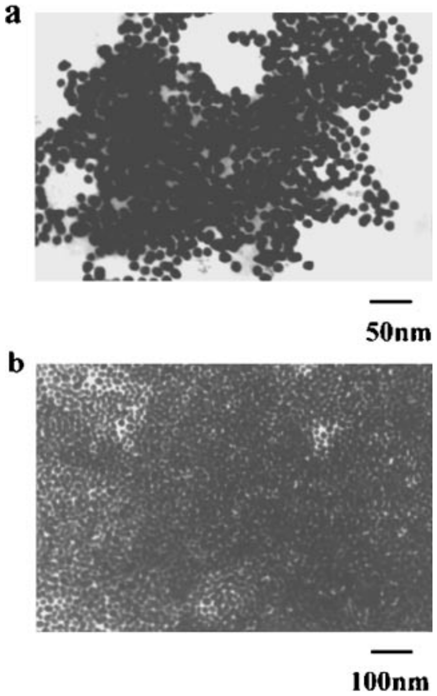

Fig. 5. TEM images of (a) and (b) show the assemblies of the colloidal Au/$HS(CH_2)_{10}$COOH at pH 11 and 3, respectively.

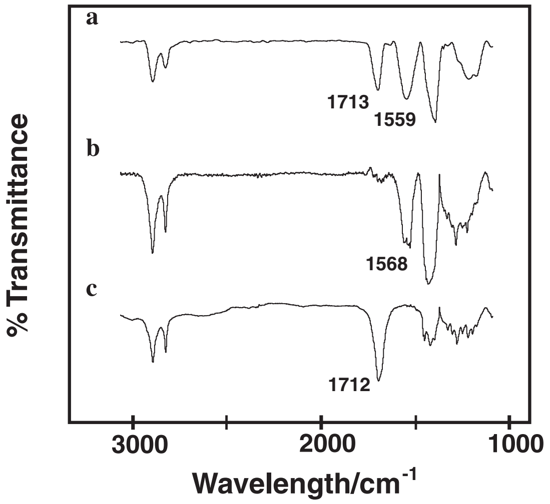

Fig. 6. FT-IR spectra attained from Au/$HS(CH_2)_{10}$COOH colloids at pH (a) 6, (b) 11, and (c) 3.

Knight shift,[17] suggesting S–H bonded to Au in the form of a thiolate bond.[17] As reported previously,[18] the ^{13}C chemical shift at 33 ppm reflects an *all-trans* conformation of the alkyl chains in a crystalline environment. On the basis of Figs. 4b–4d, both ^{13}C carboxyl resonances (–COOH and –COO$^-$) appear around 180 ppm. Therefore, the solid-state ^{13}C NMR (Fig. 4a) did not allow for a conclusion in regards to the functionalities of the modified Au colloids.

Since the Au nanoparticles can be functionalized with carboxylic acid/or carboxylate-terminated thiolates, the distinct colloidal characteristics might be changed by tuning the pH. The colloidal solutions (pH 6) were modulated using either NaOH or HCl solutions with a pH of 11 or 3, respectively. Interestingly, all solutions using those four carboxylic acids sustained the reddish color at pH 11 and showed no sign of precipitation. However, they turned purple and precipitation occurred at pH 3. Both Au nanoparticles (pH 11 and 3) showed significant 3D aggregation, as depicted in the Au/$HS(CH_2)_{10}$COOH colloids of Fig. 5. Compared with those observed at pH 11, the aggregates formed were larger and denser under acidic conditions.

To characterize the properties of the pH-modulated Au assemblies, FT-IR spectra were taken for the above three pH samples. The collected samples were washed with ethyl acetate and water before measuring the IR spectra. Figure 6a (pH 6) illustrates two characteristic peaks near 1710 and 1560 cm^{-1} corresponding to carboxylic acid dimmer and carboxylate, respectively. The carboxylate groups on the particle surfaces could lead to negatively charged colloids, resulting in repulsive interactions. Such repulsive forces would disfavor particle aggregation, which opposes hydrogen-bonding attraction in the form of the carboxylic acid groups. However, charged colloid self-assembly could be achieved through electrostatic coupling originating in the counterions localized between the nanoparticles, as shown in Scheme 1. Because the excess trisodium citrate was introduced to synthesize the Au particles in our preparation, it is highly possible that the counter ions, i.e. Na$^+$, are present among the nanocolloids. It should be mentioned that the prepared Au colloids without the addition of ω-sulfanylalkanoic or ω-alkyldisulfanylalkanoic acids showed no signals from carboxylic and carboxylate peaks. With the addition of NaOH, the pH rose to 11. Figure 6b shows only the carboxylate

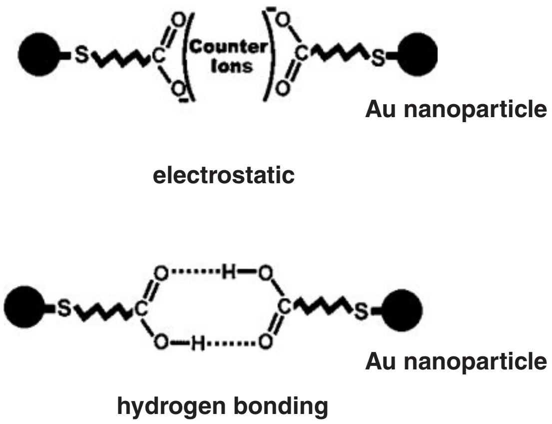

Scheme 1.

peak at 1568 cm^{-1}. Adachi has reported that the –COO$^-$ terminals facilitated Au nanospheroid assembly in the presence of counterions.[6] The existence of Na$^+$ ions indeed provided a chance to form aggregates via electrostatic attraction in this case. However, it also should be noted that the prepared Au colloids carried significant COO$^-$-terminated thiols, resulting in repulsive interactions under alkaline conditions. This results in the dispersion of the gold colloids.[4b,c] As mentioned early, we have observed that the resulting suspension remained a reddish color and exhibited good stability. Different from the observation at pH 6, TEM images showed significant 3D aggregating morphology. Based on the aforementioned consideration, it is proposed that the coagulation taking place may result from the dry-up process in the preparation of TEM samples. Herein, electrostatic interactions may play a role in aggregation during the dry-up process.[19] On the other hand, we saw the colloidal solutions turn purple and precipitate at pH 3. Figure 6c provides the evidence of the carboxylic acid standing up at 1712 cm^{-1}. In acidic solutions, interparticle interactions were governed by hydrogen bonding facilitated particle aggregation.[4a,b] The same consequences were observed in the case of the Au colloids capped with ω-alkyldisulfanylalkanoic acids at pH 3, 6, and 11 (Fig. 7).

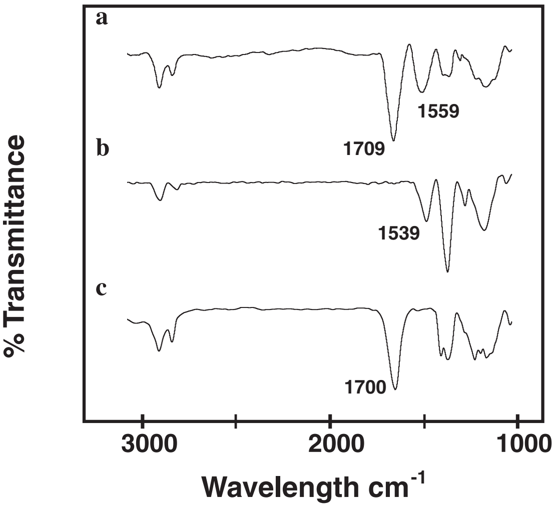

Fig. 7. FT-IR spectra attained from Au/EtSS(CH$_2$)$_{10}$COOH colloids at pH (a) 6, (b) 11, and (c) 3.

Conclusions

We have demonstrated that Au nanoparticle assemblies resulted from the simple addition of ω-sulfanylalkanoic or ω-alkyldisulfanylalkanoic acids into sodium-contained aqueous Au colloidal solutions. The resulting 2D arrays revealed the characteristics of the coexistence of both electrostatic and hydrogen-bonding attraction at pH 6. Although Au nanoparticles capped with carboxylate-terminated (–COO$^-$) thiolates could interact with Na$^+$ to lead to aggregates formation via electrostatic interactions in alkaline solutions, the observed 3D arrays might also be due to coagulation during the dry-up process in the preparation of TEM samples, considering of colloidal properties at pH 11. Under acidic conditions (pH 3), the colloidal solutions exhibited precipitation and suggested the formation of hydrogen-bonding interactions leading to 3D close-packed aggregates. Furthermore, solid-state ^{13}C NMR showed that the alkyl chains of the thiolates were present in an all-trans conformation.

Experimental

Chemicals. The following materials were obtained from Aldrich: 11-bromoundecanoic acid, 16-bromohexadecanoic acid, and thiourea. $HAuCl_4 \cdot 3H_2O$ (99.99%) was obtained from Alfa Aesar. Trisodium citrate (99.0%) was obtained from Showa. The chemicals and solvents were used as received.

Instrumentation. The transmission electron microscopy (TEM) was performed on a JOEL JEM-1200 EX instrument operating at 80 kV accelerating voltage. The UV–vis spectra were obtained using a HP 8453 UV–Visible spectrophotometer. The IR spectra were obtained using a Nicolet Magana 550 FT-IR spectrophotometer. The solution ^{1}H NMR spectra were obtained a Bruker AVANCE 300 FT-NMR spectrometer; all chemical shifts were reported in ppm from tetramethylsilane as an internal standard. The solid-state ^{13}C magic angle (MAS) NMR experiment was performed on a Bruker AVANCE 400 spectrometer, equipped with a Bruker double-tuned 7 mm probe with resonance frequencies of 100.6 MHz for ^{13}C nuclei. The Hartmann–Hahn condition for the $^1H \rightarrow {}^{13}C$ cross polarization (CP) experiment was determined using admantane. ^{13}C CP/MAS NMR spectra were recorded with a CP contact time of 3 ms, a repetition time of 4 s, and a spinning speed in 7 kHz. The ^{13}C chemical shifts were externally referenced with tetramethylsilane (TMS).

Synthesis of 11-Sulfanylundecanoic Acid ($HS(CH_2)_{10}CO_2H$). A solution of 11-bromoundecanoic acid (0.5 g, 1.9 mmol) and thiourea (0.22 g, 2.9 mmol) in water (10 mL) was refluxed for 2.5 h. Then, 5 M NaOHaq (1 M = 1 mol dm^{-3}) (4 mL) was added slowly with stirring and refluxed for another 2 h. The aqueous solution was cooled in an ice bath and acidified with hydrochloric acid to give a precipitate. After filtrating and washing with water, 11-sulfanylundecanoic acid (0.37 g, 90%) was obtained as a white powder. ^{1}H NMR ($CDCl_3$) δ 1.27 (12H, m), 1.32 (1H, t, $J = 7.5$ Hz, SH), 1.60 (4H, m), 2.34 (2H, t, $J = 7.5$ Hz), 2.51 (2H, q, $J = 7.5$ Hz).

Synthesis of 11-Ethyldisulfanylundecanoic Acid ($EtSS(CH_2)_{10}CO_2H$). A mixture of 11-sulfanylundecanoic acid (0.37 g, 1.7 mmol) and diethyl disulfide (0.42 g, 3.4 mmol) in 5 mL of triethylamine was stirred at 70 °C for 24 h. The solution was concentrated under reduced pressure followed by chromatographic purification over silica gel, eluting with CH_3OH–$CHCl_3$ (1:19) to give 11-ethyldisulfanylundecanoic acid (0.42 g, 89%). ^{1}H NMR

($CDCl_3$) δ 1.26 (12H, m) 1.29 (3H, t, $J = 7.4$ Hz), 1.61 (4H, m), 2.31 (2H, t, $J = 7.4$ Hz), 2.66 (4H, m).

Synthesis of 16-Sulfanylhexadecanoic Acid ($HS(CH_2)_{15}CO_2H$). The same procedure for the preparation of 11-sulfanylundecanoic acid was used. 16-bromohexadecanoic acid (0.5 g, 1.5 mmol) reacting with thiourea (0.17 g, 2.2 mmol) gave 16-sulfanylhexadecanoic acid (0.41 g, 95%). ^{1}H NMR ($CDCl_3$) δ 1.26 (23H, m), 1.62 (4H, m), 2.35 (2H, t, $J = 7.5$ Hz), 2.52 (2H, q, $J = 7.5$ Hz).

Synthesis of 16-Ethyldisulfanylhexadecanoic Acid ($EtSS(CH_2)_{15}CO_2H$). The same procedure for the preparation of 11-ethyldisulfanylundecanoic acid was used. 16-sulfanylhexadecanoic acid (0.41 g, 1.4 mmol) reacting with diethyl disulfide (0.35 g, 2.8 mmol) gave 16-ethyldisulfanylhexadecanoic acid (0.41 g, 85%). ^{1}H NMR ($CDCl_3$) δ 1.25 (22H, m), 1.31 (3H, t, $J = 7.4$ Hz), 1.64 (4H, m), 2.33 (2H, t, $J = 7.4$ Hz), 2.68 (4H, m).

Preparation of Functionalized Gold Nanoparticles. The Au colloids were synthesized following the method of Natan et al. by reacting 50 mL of 9.1×10^{-4} M $HAuCl_4$ with an excess of trisodium citrate in aqueous solution.[14] The 5 mL of gold colloidal aqueous solution was mixed with an ethanol solution containing 1.1 mmol of $HS(CH_2)_nCOOH$ or $EtSS(CH_2)_nCOOH$ ($n = 10$, 15). The resulting mixtures were used for UV–vis and TEM measurements. Electron micrographs of the Au colloids were carried out using a drop of the sample onto a copper mesh coated with an amorphous carbon film. This mesh was then dried in a vacuum desiccator. For solid-state ^{13}C NMR and FT-IR analysis, the collected colloidal precipitates were washed three times with ethyl acetate (5 mL) and water (5 mL) to remove the excess ω-sulfanylalkanoic or ω-alkyldisulfanylalkanoic acids.

We thank the National Science Council of the Republic of China for its financial support for this work. We also acknowledge Ms. S. Y. Hsu and Mr. S. Y. Yao for the TEM measurements and Ms. J. Z. Wu and Ms. S. Y. Sun for the solid-state NMR analysis at Tainan Regional Instrument Center, National Cheng Kung University.

References

1 A. Majetich, J. O. Artman, M. E. McHenry, N. T. Nuhfer, and S. W. Staley, *Phys. Rev. B: Condens. Matter*, **48**, 16845 (1993).

2 J. J. Storhoff, R. Elghanian, R. C. Mucic, C. A. Mirkin, and R. L. Lestinger, *J. Am. Chem. Soc.*, **120**, 1959 (1998).

3 See for example: a) S. L. Tripp and A. Wei, *J. Am. Chem. Soc.*, **123**, 7955 (2001). b) M. Gianini, W. R. Caseri, and U. W. Suter, *J. Phys. Chem. B*, **105**, 7399 (2001). c) Z. L. Wang, *Adv. Mater.*, **10**, 13 (1998). d) Z. L. Wang, S. A. Harfenist, R. L. Whetten, J. Bentley, and N. D. Evans, *J. Phys. Chem. B*, **102**, 3068 (1998). e) L. Motte, F. Billoudet, and M. P. Pileni, *J. Phys. Chem.*, **99**, 16425 (1995).

4 See for example: a) Y. Shiraishi, D. Arakawa, and N. Toshima, *Eur. Phys. J. E*, **8**, 377 (2002). b) J. Simard, C. Briggs, A. K. Boal, and V. M. Rotello, *Chem. Commun.*, **2000**, 1943. c) W. Zhong, M. M. Maye, F. L. Leibowitz, and C. J. Zhong, *Anal. Chem.*, **72**, 2190 (2000). d) A. C. Templeton, D. E. Cliffel, and R. W. Murray, *J. Am. Chem. Soc.*, **121**, 7081 (1999). e) S. Gomez, L. Erades, K. Philippot, B. Chaudret, V. Colliére, O. Balmes, and J.-O. Bovin, *Chem. Commun.*, **2001**, 1474. f) A. K. Boal, F. Ilhan, J. E. DeRouchey, T. Thurm-Albrecht, T. P. Russell, and V. M. Rotello, *Nature*, **404**, 746 (2000). g) A. K. Boal and V. M. Rotello, *Langmuir*, **16**, 9527 (2000). h) L. Cusack, R. Rizza, A. Gorelov, and D. Fitzmaurice, *Angew. Chem., Int. Ed. Engl.*, **36**, 848 (1997).

5 D. G. Grier, *Nature*, **393**, 621 (1998).

6 E. Adachi, *Langmuir*, **16**, 6460 (2000).

7 J. Kolny, A. Kornowski, and H. Weller, *Nano Lett.*, **2**, 361 (2002).

8 W. C. W. Chan and S. Nie, *Science*, **281**, 2016 (1998).

9 G. P. Mitchell, C. A. Mirkin, and R. L. Lestinger, *J. Am. Chem. Soc.*, **121**, 8122 (1999).

10 S. R. Johnson, S. D. Evans, and R. Brydson, *Langmuir*, **14**, 6639 (1998).

11 S. Chen and K. Kimura, *Langmuir*, **15**, 1075 (1999).

12 H. Yao, O. Momozawa, T. Hamatani, and K. Kimura, *Chem. Mater.*, **13**, 4692 (2001).

13 C. S. Weisbecker, M. V. Merritt, and G. H. Whitesides, *Langmuir*, **12**, 3763 (1996).

14 C. Grabar, R. G. Freeman, M. B. Hommer, and M. J. Natan, *Anal. Chem.*, **67**, 735 (1995).

15 R. H. Terrill, T. A. Postlethwaite, C. H. Chen, C. D. Poon, A. Terzis, A. Chen, J. E. Hutchison, M. R. Clark, G. Wignall, J. D. Londono, R. Superfine, M. Falvo, C. S. Johnson, E. T. Samulski, and R. W. Murray, *J. Am. Chem. Soc.*, **117**, 12537 (1995).

16 See for example: a) A. Ulman, *Chem. Rev.*, **96**, 1533 (1996). b) A. Badia, L. Demers, L. Dickinson, F. G. Morin, R. B. Lennox, and L. Reven, *J. Am. Chem. Soc.*, **119**, 11104 (1997). c) J. Noh, T. Murase, K. Nakajima, H. Lee, and M. Hara, *J. Phys. Chem. B*, **104**, 7411 (2000).

17 See for example: a) A. Badia, W. Gao, S. Singh, L. Cuccia, and L. Reven, *Langmuir*, **12**, 1262 (1996). b) B. S. Zelakiewicz, A. C. de Diol, and Y. Y. Tong, *J. Am. Chem. Soc.*, **125**, 18 (2003).

18 H. Schmitt, A. Badia, L. Dickinson, L. Reven, and R. B. Lennox, *Adv. Mater.*, **10**, 475 (1998).

19 We acknowledge the editor and reviewer for the insightful comments.